Journal of Geosciences and Geomatics, 2017, Vol. 5, No. 3, 119-129
Available online at http://pubs.sciepub.com/jgg/5/3/3

DOI:10.12691/jgg-5-3-3

The Pan-African Biotite-Muscovite Granite and Amphibole-Biotite Granite of Doua (Central Cameroon): Zircon Features, LA-MC-ICP-MS U-Pb Dating and Implication on Their Tectonic Setting

Amadou Diguim Kepnamou[1], Ganwa Alembert Alexandre[1,2,*], Klötzli Urs[2], Hauzenberger Christoph[3], Ngounouno Ismaïla[1], Naïmou Seguem[1,4]

[1]Department of Earth Sciences, Faculty of Sciences, University of Ngaoundere, PoBox 454 Ngaoundere, Cameroon
[2]Labor für Geochronologie, Department für Lithosphärenforschung, Universität Wien, Althanstrasse 14, 1090 Wien, Austria
[3]Institut für Erdwissenschaften, Bereich Mineralogie & Petrologie, A-8010 Graz, Universitätsplaz 2/2.Stock, Austria
[4]Department of Geology, Faculty of Sciences and Techniques, University Adam Barka of Abeche, Abeche, Chad
*Corresponding author: ganwa1@yahoo.fr, alembert.alexandre.ganwa@univie.ac.at

Abstract The Doua area belongs to the Adamawa-Yadé domain (AYD) of the Central African Fold Belt (CAFB) in Cameroon. It is crossed by the Central Cameroonian Shear Zone (CCSZ). The purpose of this research is to determine the tectonic setting of granites of the studied area, based on their petrography, zircons feature and their ages. Petrographicaly, the Doua area is made up of plutonic rocks hosted in an ortho or paraderivative metamorphic basement. Amphibole-biotite granite (ABG) and biotite-muscovite granite form hills and crop out on the hill side, as flagstones in the valley or river bed, and as huge blocks. Amphibole-biotite granite is granular in texture and made up of amphibole, biotite, feldspar, accessory minerals (Sphene, zircon, and apatite) and secondary minerals (sericite). Biotite-muscovite granite (BMG) is granular to granular porphyritic in texture, made up of biotite, muscovite, plagioclase, K-feldspar, quartz, accessory minerals (zircon, opaques minerals) and secondary minerals (chlorite, sericite). ABG show elongated zircon grains with well-developed magmatic oscillatory zonation. LA-ICP-MS U-Pb data from these zircons define a concordia age of 607 ± 3 Ma and considered as crystallization age of the granite. BMG shows zircon with various shape and various internal structures (oscillatory zonation, sector zonation, blurred oscillatory zonation …) which are divided into two sets. The first set regarded as xenocryst from Paleoproterozoic granitoids emplaced at 2126 ±36 Ma or from sediments which detritus comes from such granitoids. The second set of zircons shows effects of recent lead lost and a subconcordant U-Pb age of 646 ± 39 Ma . ABG was emplaced during the D3 deformational phase, date at 607 ± 3 Ma , while BMG was trigger because of syn-D1 activity of the CCSZ at 647 ±46 Ma in association with the collisional process.

Keywords: *zircon features, U-Pb ages, granites, Doua, continental collision, central african fold belt*

Cite This Article: Amadou Diguim Kepnamou, Ganwa Alembert Alexandre, Klötzli Urs, Hauzenberger Christoph, Ngounouno Ismaïla, and Naïmou Seguem, "The Pan-African Biotite-Muscovite Granite and Amphibole-Biotite Granite of Doua (Central Cameroon): Zircon Features, LA-MC-ICP-MS U-Pb Dating and Implication on Their Tectonic Setting." *Journal of Geosciences and Geomatics*, vol. 5, no. 3 (2017): 119-129. doi: 10.12691/jgg-5-3-3.

1. Introduction

The Central African Fold Belt (CAFB, Figure 1) is classicaly subdivided into three main lithostructural domains [16,18,32]. Between the West Cameroon Domain (WCD) and the Yaounde Domain (YD) lies the Adamawa Yade Domain (AYD). The AYD is characterized by the abundance of syn to late tectonic granitoidic rocks [1,9] and the regional transcurent shear zone among which the Tcholliré Banyo Shear Zone (TBSZ), the Central Cameroon Shear Zone (CCSZ), the Sanaga Shear Zone (SSZ). Petrological, geochemical, tectonical and geochronological investigation have been carry out in granitoids of central Cameroon, part of the Adamawa Yade domain [4,17,19,30]. Despite these numerous works, many areas still unexplored and it is difficult in the present state of knowledge to decipher the number of successive generation of granitoids during the Pan-African orogeny in central Cameroon. In the present paper, we present petrography, zircon feature and Th-U-Pb data of biotite-muscovite granite and associated amphibole-biotite granite. We then deduce the implication on their geodynamic setting.

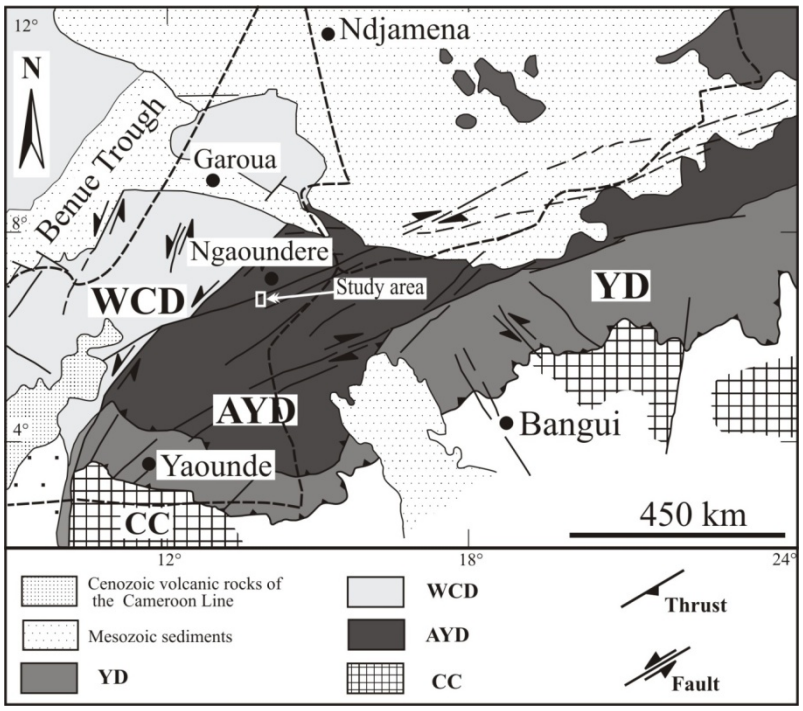

Figure 1. Geological sketch map of central Africa Fold Belt (CAFB) showing the study area (redrawn after [32]). **WCD:** West Cameroon Domain; **AYD :** Adamawa-Yade Domain ; **YD :** Yaoundé Domain ; **CC:** Congo Craton

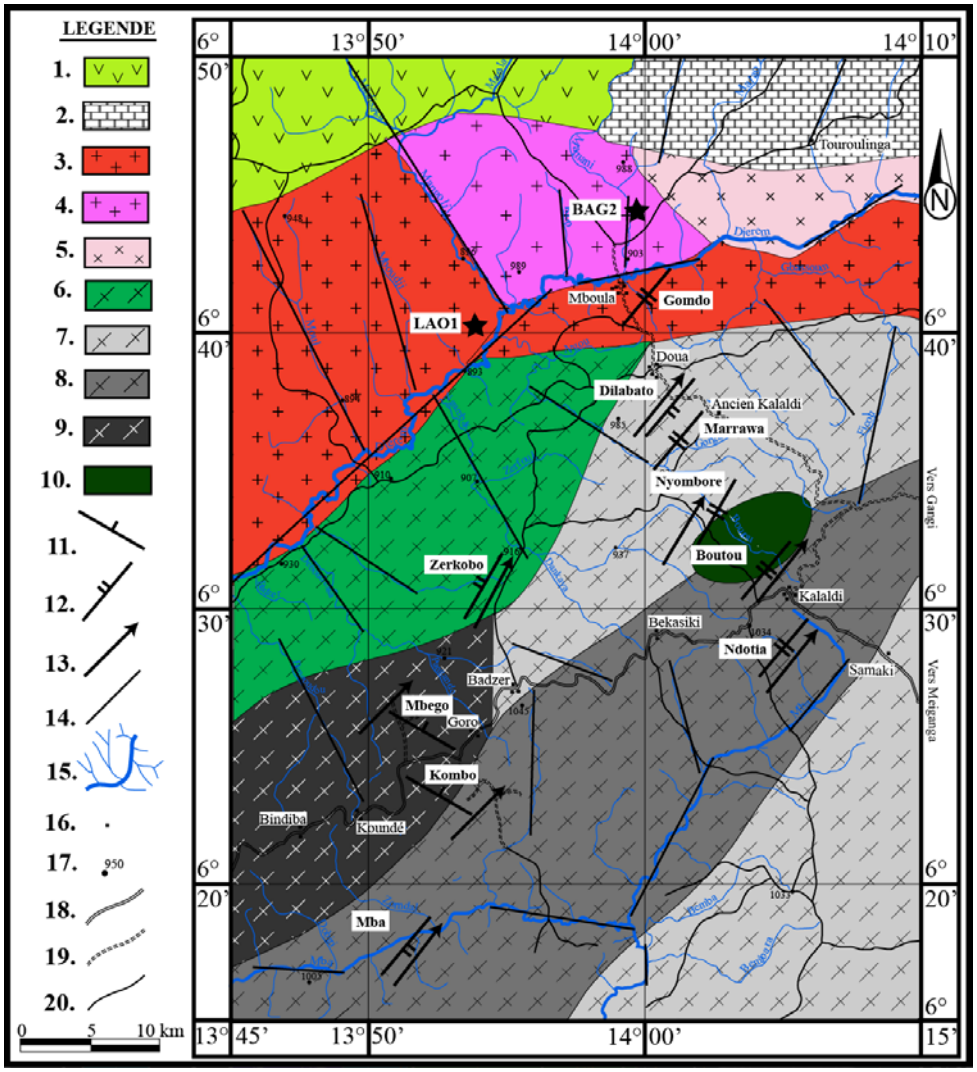

Figure 2. Geological map of the Doua-Kalaldi-Badzer area**. 1**- Basalt ; **2**- Sandstone ; **3**- Amphibole-biotite granite ; **4**- Biotite-muscovite granite ; **5**- Syenite ; **6**- Orthogneiss ; 7- Amphibole gneiss; **8**- Amphibole-biotite gneiss ; **9**- Biotite gneiss; **10**- Amphibolite ; **11**- S1 Foliation ; **12**- S2 Schistosity ; **13**- L2 Lineation, **14**- Fracture ; **15**- Rivers ; **16**- Localities ; **17**- height spot ; **18**- Main road ; **19**- Secondary road, **20**- Path

2. Geological Setting

Doua area (Figure 2) is part of the Adamawa Yade domain in central Cameroon, very close to the central cameroonian shear zone. Central Cameroon is characterized by widespread of granitoids, many in close association to the transcurrent shear zone [3,17]. The hosted rocks are ortho- and paraderivative gneisses, of various composition (Amphibole biotite gneiss, biotite gneiss), of Paleoproterozoic ages [1,20]. They have been considered as belonging to the West Central African Fold Belt and which have been reworking during the panafrican orogeny at Neoproterozoic (Penaye et al. 2004). The paleoproterozoic ages referred to igneous and contemporary metamorphic ages. Archean crustal inheritances have been demonstrated in these rocks [2,16]. In Ngaoundere, granitoids are amphibole biotite granite, biotite granite and biotite and muscovite granite of mantle and crustal origin respectively [30]. In the Meiganga area, granitoids are amphibole biotite granite, biotite muscovite granite, metadiorite with metaluminous to slightly peraluminous in character [3]. They show crustal, mantle, and/or metabasalt or metatonalite melt signature. Emplacement and cristallisation of metadiorite and pyroxene-amphibole-biotite granite was date at 614-619 Ma and 601 ± 1 Ma respectively (Lead evaporation ages, [1]). In Tibati area, diorite, tonalite, granodiorite and granite form four plutons, emplaced in close association with central Cameroon Shear Zone [17]. In Ngaoundere, granitoids are made up of hornblende-biotite granitoids, generated by magma from subcontinental lithospheric mantle, biotite granitoid and biotite –muscovite granitoid, both probably derived from melting of middle continental crust [30].

3. Analytical Techniques

3.1. Mineral Separation

Zircons were extracted by conventional mineral separation using crushing, sieving, shaking table, heavy liquid and manual separation. Highest quality zircons were mounted in 1-inch epoxy resin discs, grinded and polished to median sections and investigated by SEM-CL imaging to reveal internal chemical zonation features.

3.2. Laser-ablation MC-ICP-MS

The LA-ICP-MS (laser-ablation microprobe - inductively coupled plasma - mass spectrometry) analytical work was performed at the Laboratory of Technische Universität Graz, Austria. Analytical procedures were identical to the methodology outlined in [8]: Zircon $^{206}Pb/^{238}U$ and $^{207}Pb/^{206}Pb$ ages were determined using a 193nm solid state Nd-YAG laser (NewWave UP193 Excimer) coupled to a multi-collector ICP-MS (Nu Instruments; Nu Plasma II). Ablation using He as carrier gas was raster-wise according to the CL zonation pattern of the zircons. Line widths for rastering were 10 µm with a rastering speed of 5 µm/sec. Energy densities were 5 – 8 J/cm2 with a repetition rate of 10 Hz. The He carrier gas was mixed with the Ar carrier gas flow prior to the ICP plasma torch. Ablation duration was 60 to 120 sec with a 30 sec gas and Hg blank count rate measurement preceding ablation. Ablation count rates were corrected accordingly offline. Remaining counts on mass 204 were interpreted as representing ^{204}Pb. Static mass spectrometer analysis was as follows: ^{238}U in a Faraday detector, ^{207}Pb, ^{206}Pb, and 204 (Pb+Hg) were in ion counter detectors. ^{208}Pb was not analysed. An integration time of 1 sec was used for all measurements. The ion counter – Faraday and inter-ion counter gain factors were determined before the analytical session using reference zircon Plesovice [27]. Sensitivity for ^{206}Pb on reference zircon Plesovice was c. 30’000 cps/ppm Pb. For ^{238}U the corresponding value was c. 35'000 cps/ppm U.

Mass and elemental bias and mass spectrometer drift of both U/Pb and Pb/Pb ratios, respectively, were corrected using a multi-step approach: first-order mass bias is corrected using a dried ^{233}U-^{205}Tl-^{203}Tl spike solution which was aspirated continuously in Ar and mixed to the He carrier gas coming from the laser before entering the plasma. This corrects for bias effects stemming from the mass spectrometer. The strongly time-dependent elemental fractionation stemming from the ablation process is corrected for using the "intercept method" of [29]. The calculated $^{206}Pb/^{238}U$ and $^{207}Pb/^{206}Pb$ intercept values are corrected for mass discrimination from analyses of reference zircon Plesovice measured during the analytical session using a standard bracketing method [7]. The correction utilizes regression of standard measurements by a quadratic function. A common Pb correction was applied to the final data using the apparent $^{207}Pb/^{206}Pb$ age and the Stacey and Kramers [28] Pb evolution model. Final age calculations were performed with Isoplot© 3.0 [11]. All errors reported for LA data are at the 2-sigma level.

4. Results

4.1. Petrography of the Study Samples

The studied rocks are located in the Doua area (Figure 2). Amphibole-bioite granite (ABG) crop out on the hills west of Doua village (Figure 3a). It shows frequently amphibolite enclave (Figure 3b). The rock is granular in texture (Figure 3c) and made up of amphibole, biotite, Feldspar, quartz, accessory minerals (sphen, zircon, apatite), opaque mineral and secondary minerals (cericite). Amphibole is a green hornblende of variable size (1 to 6 mm long), with inclusions of zircon, apatite, opaques (Figure 3d), and portrays sometime Carlsbad twin system. Amphibole is associated to brownish biotite which is sometime transformed into chlorite and opaque mineral. Feldspar is constituted of plagioclase and K-feldspar. Plagioclase displays regularly combined albite and Carlsbad twining. Albite twin is sometime beveled in the mineral. Some crystals are affected by ceritization. Plagioclase is associated to quartz and K-feldspar. K-feldspar is perthitic, with film exsolutions sub perpendicular to the elongation of the crystal. Bourgeons of myrmeckite usually growth at the border of the Kfeldspar.

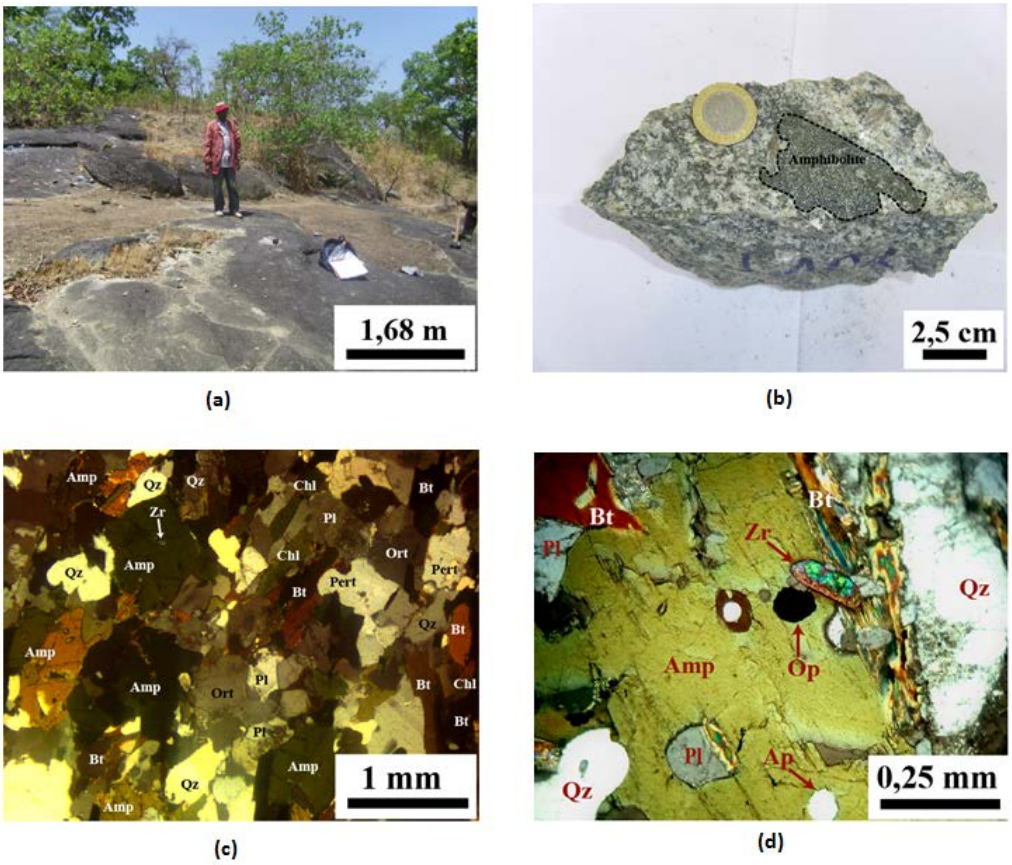

Figure 3. (**a)** Outcrop of the amphibole-biotite granite ; (**b)** Amphibole-biotite granite sample showing an enclave of amphibolite ; **(c) –** Photomicrograph in plain-polarized light showing the granular texture of the ABG; (**d)-** Association amphibole, apatite, zircon, opaque, quartz, plagiolsase (plain-polarized light)

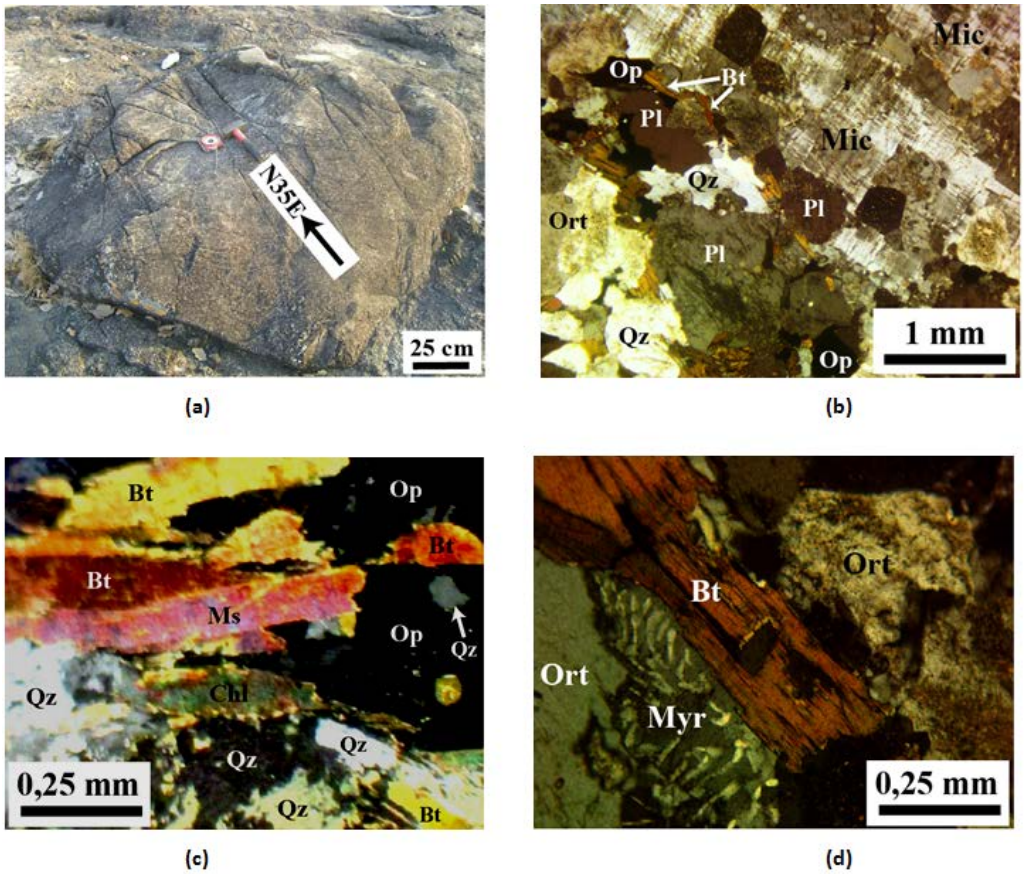

Figure 4. a- Cracked block of biotite-muscovite granite at the top of Baggo hill; **b-** Photomicrograph in plain-polarized light showing the porphyritic granular texture of the biotite-muscovite granite; **c-** Photomicrograph in plain-polarized light showing association of muscovite, biotite, quartz and opaque minerals; **d-** Biotite flake associated to K-feldspar (orthoclase) under plain polarized light

Biotite-muscovite granite (BMG) crops out at the top of the Baggo hill, as flat stones surmounted by huge decametric blocks (Figure 4a). It shows granular to granular porphyritic in texture (Figure 4b) made up of biotite, muscovite, plagioclase, K-feldspar, quartz, accessory minerals (zircon, opaque minerals), and secondary minerals (chlorite, sericite). The rock shows fain schistosity with the aligment of biotite. Biotite forms brownish flake of 0.8 to 1.2 mm long, associated to feldspar, muscovite of the same size (Figure 4c) and opaque minerals. Quartz is subhedral with ondulose extinction and sometime grouped into many crystals. Plagioclase usually combines albite and carlbad twins. It is associated to Kfeldspar and is being transformed into sericite. K-feldspar is made up of perthitic orthoclase with flaming albitic exsolution, and microcline. K-feldspar regularly shows myrmeckitic intergrowth at its border (Figure 4d). Opaque minerals are associated to other minerals of the rocks and sometine in inclusion in feldspar.

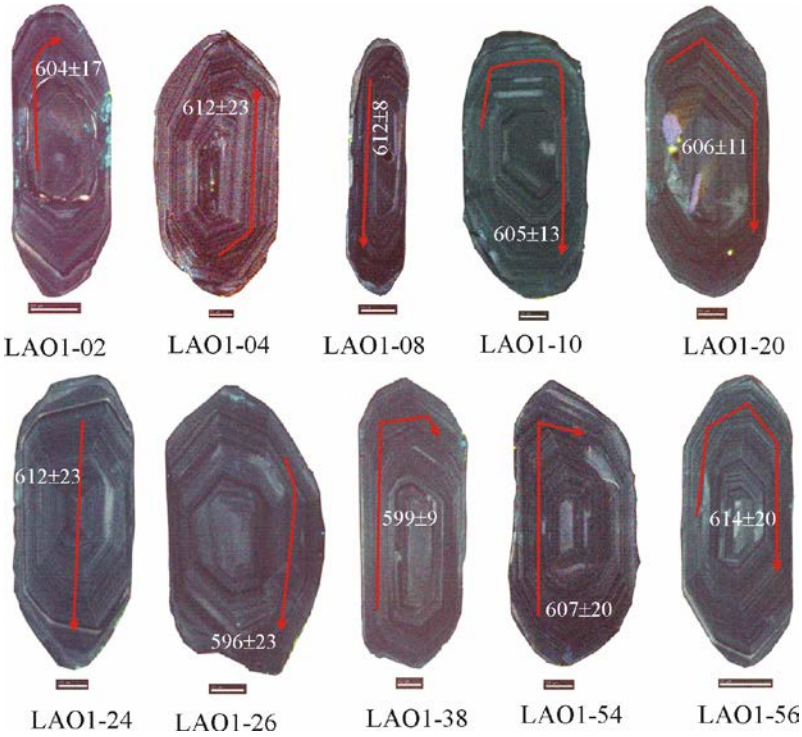

Figure 5. Cathodoluminescence images of selected zircons of ABG (sample LAO1). The red arrows show the approximate location of the laser ablation trenches

Figure 6. Cathodoluminescence images of selected zircons of the BMG (sample BAG2). The arrows show the approximate location of the laser ablation trenches

4.2. Zircon Feature

The amphibole-biotite granite has zircon grains characterized with few exceptions by length/wide ratio of approximately 2.5/1. The internal structure of representative grains is shown in Figure 5. They show well developed magmatic oscillatory zonation. Some zircons have elongated to sub roundish inclusions (e.g. LAO-08, LAO1-20).

The biotite-muscovite granite shows elongated and stubby zircons with length/wide ratio of 2.5/1 (e.g. BAG2-02, BAG2-04, BAG2-12) and 1.5/1 (e.g. BAG2-10, BAG2-60, BAG2-72) respectively. Internal structure of representative zircons can be seen in Figure 6. They are characterized by two domains, an inner part and an outer part. The outer domains show oscillatory zonation with alternation of thick CL no emission and CL bright layers. This zonation is sometime convolute (e.g BAG2-02). The inner part is characterized sector zonation (BAG2-60, BAG2-72, BAG2-74), blurred oscillatory zonation (BAG2-14, BAG2-18, BAG2-40, BAG2-48), or no zonation (BAG2-04, BAG2-10, BAG2-12). Outer part of zircon grains is separated from the inner part by a more or less thick CL bright band. This band is regularly transgresses in the inner part of the grain (e.g. BAG2-12, BAG2-14, BAG2-48).

4.3. U-Pb isotopic Analysis of Zircons

A total of 21 LA-ICP-MS U–Pb analyses were performed including 10 in 10 zircons of the ABG and 11 in 11 zircons of the BMG. These data are summarized in the Table 1. ABG sample (LAO1) shows $^{206}Pb/^{238}U$ and $^{207}Pb/^{206}Pb$ apparent ages ranging from 596 ± 4 Ma to 614 ± 3 Ma, and 600 ± 1 Ma to 634 ± 5 Ma respectively. A plot of these zircon data portrays a Concordia age of 607 ± 3 Ma (Figure 7).

The $^{206}Pb/^{238}U$ and $^{207}Pb/^{206}Pb$ apparent ages vary from 2326 ± 2 Ma (Siderian) to 565 ± 4 Ma (Ediacaran), and 2146 ±0.5 Ma (Rhyacian) to 585 ± 6 Ma (Ediacaran). A concordia plot of all zircon grains data of the BMG sample (BAG2) portrays a Discordia line with an upper intercept at 2123 ± 52 Ma (Rhyacian) and lower intercept at 610 ±57 Ma (Ediacaran, Figure 8). With respect to $^{206}Pb/^{238}U$ ratio, two groups of data are distinguish: data with ratio superior to 0.3 and data with ratio inferior to 0.3. In the Concordia plot, the first group of data defines a Discordia line (Figure 9) with Rhyacian upper intercept (2126 ± 36 Ma) and Cryogenian lower intercept (667 ± 46 Ma); zircon grain BAG2-18 is in a reverse discordancy, which is difficult to understand in a local geological context. Nevertheless, we do not discard it because at the error limit, it has no influence on the result. The second group defines a discordia line with upper intercept at 647 ± 46 Ma (Cryogenian) and lower intercept at 6 ± 530 Ma (plot not schown). We consider the lower intercept as being due to recent lead loss; therefore, we anchored the lower intercept at a more realistic and better constrained age, 1 ±0.5 Ma and therefore, the upper intercept becomes 646 ±39 Ma (Figure 10). The data of the first group are obtain in a rastering line located in the inner part of the grain (BAG2-18, BAG2-38, BAG2-48) except the data of one zircon (BAG2-70). Data of the second group are obtained mainly from the outer domains of zircon.

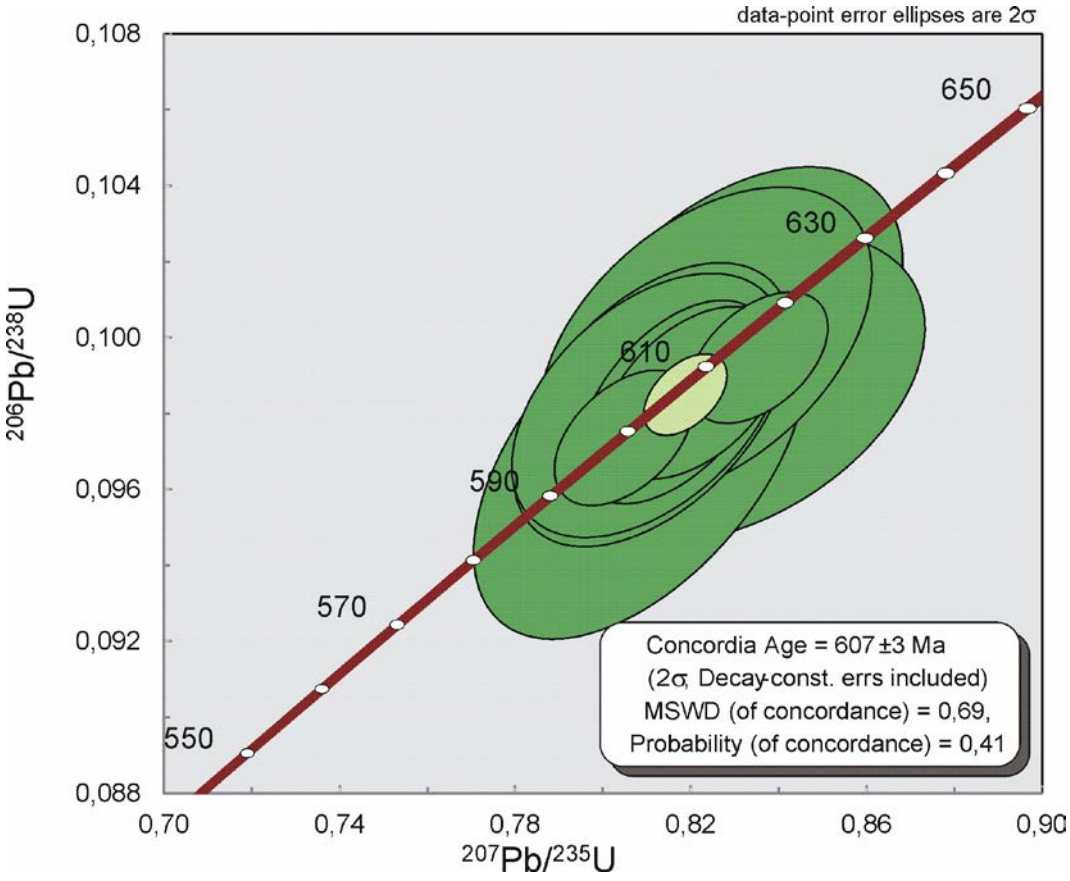

Figure 7. Concordia plot with the data of all selected zircons of LAO1 granite sample

Table 1. U-Pb analytical results from zircons of ABG and BMG

Sample	Crystal	n° counting	Zircon CL pattern	BLANK CORRECTED INTENSITIES (in V)						STANDARD CORRECTED RATIOS	
				204Pb	206Pb	207Pb	208Pb	232Th	238U	206Pb / 204Pb	2RSE (%)
LAO1 (ABG)	038	198	OZ	3,83E-06	3,08E-03	1,82E-04	8,32E-04	2,35E-02	3,75E-02	765	3,47
	026	164	OZ	4,06E-06	2,44E-03	1,45E-04	6,40E-04	1,75E-02	2,81E-02	848	3,86
	002	184	OZ	4,56E-06	2,52E-03	1,49E-04	5,63E-04	1,23E-02	2,21E-02	651	2,97
	024	175	OZ	3,78E-06	3,32E-03	1,96E-04	1,16E-03	3,34E-02	3,86E-02	988	2,52
	010	181	OZ	4,40E-06	2,93E-03	1,73E-04	8,90E-04	2,53E-02	3,38E-02	891	1,39
	020	190	OZ	3,79E-06	3,26E-03	1,95E-04	9,42E-04	2,71E-02	3,80E-02	968	1,82
	056	149	OZ	3,54E-06	2,59E-03	1,53E-04	6,76E-04	1,85E-02	3,03E-02	829	4,35
	004	151	OZ	3,79E-06	2,06E-03	1,22E-04	4,87E-04	1,35E-02	2,35E-02	635	7,50
	054	174	OZ	4,15E-06	2,78E-03	1,69E-04	8,51E-04	2,33E-02	3,23E-02	791	3,36
	008	201	OZ	4,44E-06	3,12E-03	1,87E-04	9,07E-04	2,51E-02	3,62E-02	677	1,02
BAG2 (BMG)	040	265	BlOZ	4,89E-06	2,00E-03	1,38E-04	3,22E-04	8,31E-03	2,28E-02	902	2,07
	014	105	BlOZ	5,95E-06	1,76E-02	1,09E-03	3,59E-03	9,73E-02	2,06E-01	5587	10,90
	060	172	SZBlOZ	2,73E-06	1,40E-03	8,24E-05	2,02E-04	5,20E-03	1,49E-02	1024	3,98
	072	207	SZ	2,82E-06	4,93E-03	2,97E-04	5,49E-05	1,15E-03	4,96E-02	3684	8,44
	006	86	OZ	1,82E-06	4,40E-03	3,25E-04	3,95E-04	1,00E-02	4,65E-02	4024	17,76
	002	81	BlOZ	2,68E-06	6,87E-03	4,44E-04	1,41E-03	2,93E-02	7,23E-02	4527	43,90
	074	203	BlOZ	2,47E-06	4,80E-03	2,90E-04	7,31E-04	1,75E-02	4,94E-02	4578	8,37
	048	188	BlOZSZ	6,31E-06	1,32E-03	8,90E-05	6,15E-04	1,40E-02	1,31E-02	179	1,71
	038	146	SZBlOZ	2,68E-06	2,09E-03	2,67E-04	5,34E-04	4,37E-03	6,73E-03	1561	2,92
	070	240	OZ	3,85E-06	4,80E-03	6,27E-04	3,46E-04	2,38E-03	1,41E-02	2490	6,40
	018	177	SZBlOZ	2,84E-06	3,08E-03	3,99E-04	4,13E-04	3,50E-03	8,46E-03	1634	6,77

Sample	Crystal	n° counting	Zircon CL pattern	STANDARD CORRECTED RATIOS							
				207Pb / 235U	2RSE (%)	206Pb / 238U	2RSE (%)	Rho	207Pb / 206Pb	2RSE (%)	208Pb / 206Pb
LAO1 (ABG)	038	198	OZ	0,8047	1,61	0,0974	1,50	0,47	0,0600	0,32	0,7180
	026	164	OZ	0,8085	3,84	0,0969	4,05	0,53	0,0604	0,32	0,7453
	002	184	OZ	0,8103	3,14	0,0982	2,90	0,46	0,0599	0,29	0,6210
	024	175	OZ	0,8112	3,19	0,0983	3,12	0,49	0,0599	0,26	1,0066
	010	181	OZ	0,8161	2,17	0,0983	2,23	0,51	0,0601	0,25	0,8407
	020	190	OZ	0,8205	2,03	0,0986	1,89	0,46	0,0606	0,44	0,8633
	056	149	OZ	0,8234	3,76	0,0999	3,38	0,45	0,0600	0,44	0,7844
	004	151	OZ	0,8267	4,11	0,0997	4,00	0,49	0,0601	0,47	0,5430
	054	174	OZ	0,8296	4,32	0,0987	3,39	0,39	0,0608	1,53	0,9893
	008	201	OZ	0,8355	1,54	0,0995	1,42	0,46	0,0609	0,26	0,6470
BAG2 (BMG)	040	265	BlOZ	0,7712	3,84	0,0917	2,42	0,31	0,0619	2,08	0,5342
	014	105	BlOZ	0,7837	4,83	0,0917	3,95	0,41	0,0614	2,05	0,5651
	060	172	SZBlOZ	0,7988	4,54	0,0968	4,49	0,49	0,0598	0,41	0,4680
	072	207	SZ	0,8999	3,35	0,1058	3,50	0,52	0,0614	0,39	0,0399
	006	86	OZ	0,9528	32,32	0,0976	15,49	0,24	0,0621	10,20	0,2948
	002	81	BlOZ	0,9646	11,00	0,1077	10,34	0,47	0,0651	4,47	0,7123
	074	203	BlOZ	0,9952	5,19	0,1199	5,33	0,51	0,0595	1,56	0,5179
	048	188	BlOZSZ	1,2100	5,39	0,1220	2,70	0,25	0,0690	3,54	1,3596
	038	146	SZBlOZ	5,9759	3,10	0,3340	3,07	0,50	0,1300	0,33	0,8386
	070	240	OZ	6,9267	2,18	0,3833	2,02	0,46	0,1306	0,61	0,2101
	018	177	SZBlOZ	8,0205	2,78	0,4344	2,78	0,50	0,1336	0,55	0,4815

Sample	Crystal	n° counting	Zircon CL pattern	STANDARD CORRECTED RATIOS				Apparent Age			
				2RSE (%)	208Pb / 232Th	2RSE (%)	232Th 238U	206Pb / 238U	2RSE (%)	207Pb / 206Pb	2RSE (%)
LAO1 (ABG)	038	198	OZ	6,31	0,0305	1,70	0,63	599	1,43	605	1,15
	026	164	OZ	2,97	0,0296	4,16	0,62	596	3,86	616	1,12
	002	184	OZ	2,72	0,0296	2,73	0,56	604	2,76	600	1,03
	024	175	OZ	5,02	0,0287	3,89	0,86	604	2,97	600	0,94
	010	181	OZ	2,92	0,0291	2,28	0,75	605	2,13	608	0,88
	020	190	OZ	2,62	0,0292	2,00	0,71	606	1,80	626	1,50
	056	149	OZ	4,31	0,0314	2,64	0,61	614	3,22	602	1,59
	004	151	OZ	11,93	0,0294	4,88	0,57	612	3,81	607	1,67
	054	174	OZ	4,41	0,0305	3,57	0,72	607	3,23	634	5,15
	008	201	OZ	8,19	0,0310	1,08	0,70	612	1,36	634	0,88
BAG2 (BMG)	040	265	BlOZ	4,07	0,0264	4,36	0,36	565	2,31	669	6,55
	014	105	BlOZ	9,08	0,0303	4,68	0,47	565	3,77	652	6,67
	060	172	SZBlOZ	1,32	0,0278	5,12	0,35	595	4,28	597	1,47
	072	207	SZ	6,62	0,0385	4,14	0,02	648	3,33	652	1,27
	006	86	OZ	8,43	0,0318	16,02	0,22	600	14,69	677	30,16
	002	81	BlOZ	17,62	0,0418	12,55	0,41	659	9,78	779	11,72
	074	203	BlOZ	7,19	0,0381	8,32	0,35	730	5,02	585	5,74
	048	188	BlOZSZ	5,03	0,0405	4,95	1,07	742	2,55	899	7,92
	038	146	SZBlOZ	2,58	0,0962	2,75	0,65	1858	2,66	2098	0,27
	070	240	OZ	4,06	0,1081	3,67	0,17	2091	1,72	2106	0,51
	018	177	SZBlOZ	6,67	0,1077	4,06	0,41	2326	2,32	2146	0,45

O: Oscillatory; Z: Zonation; S: Sector; Bl: Blured.

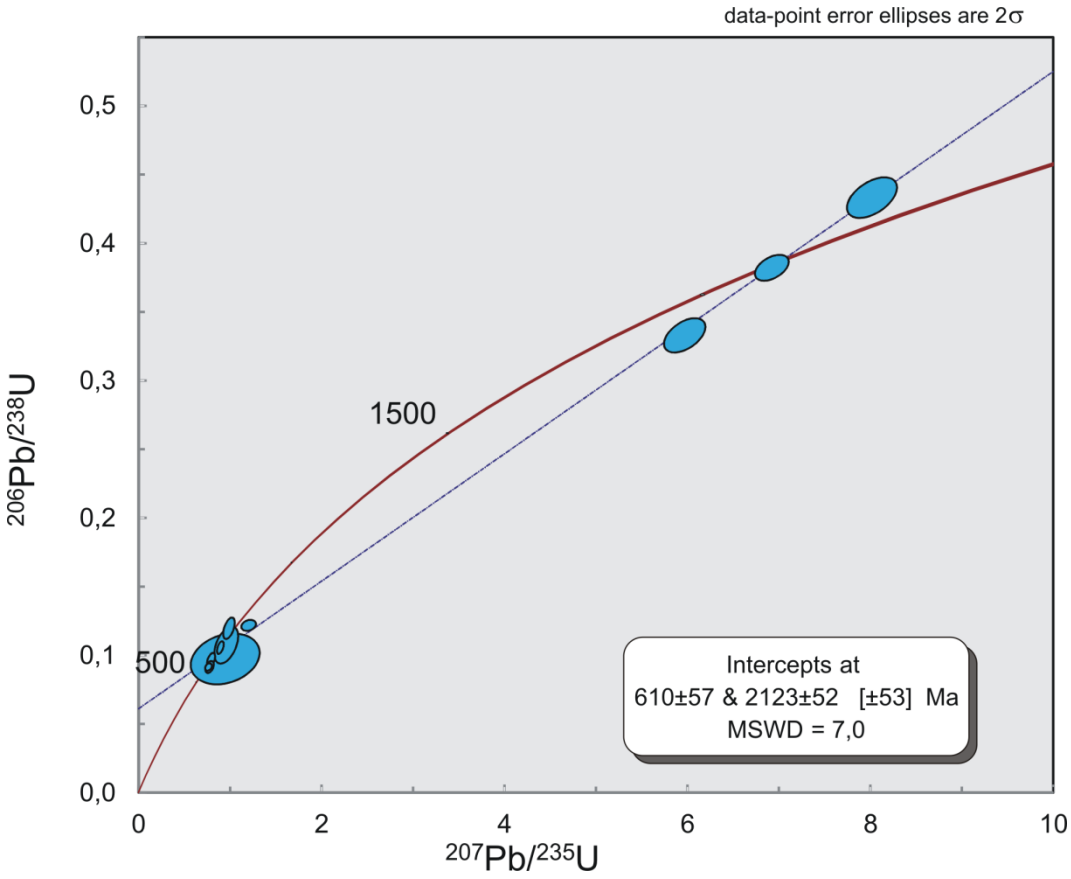

Figure 8. Concordia plot with the data of all selected zircons of BAG2 BMG sample

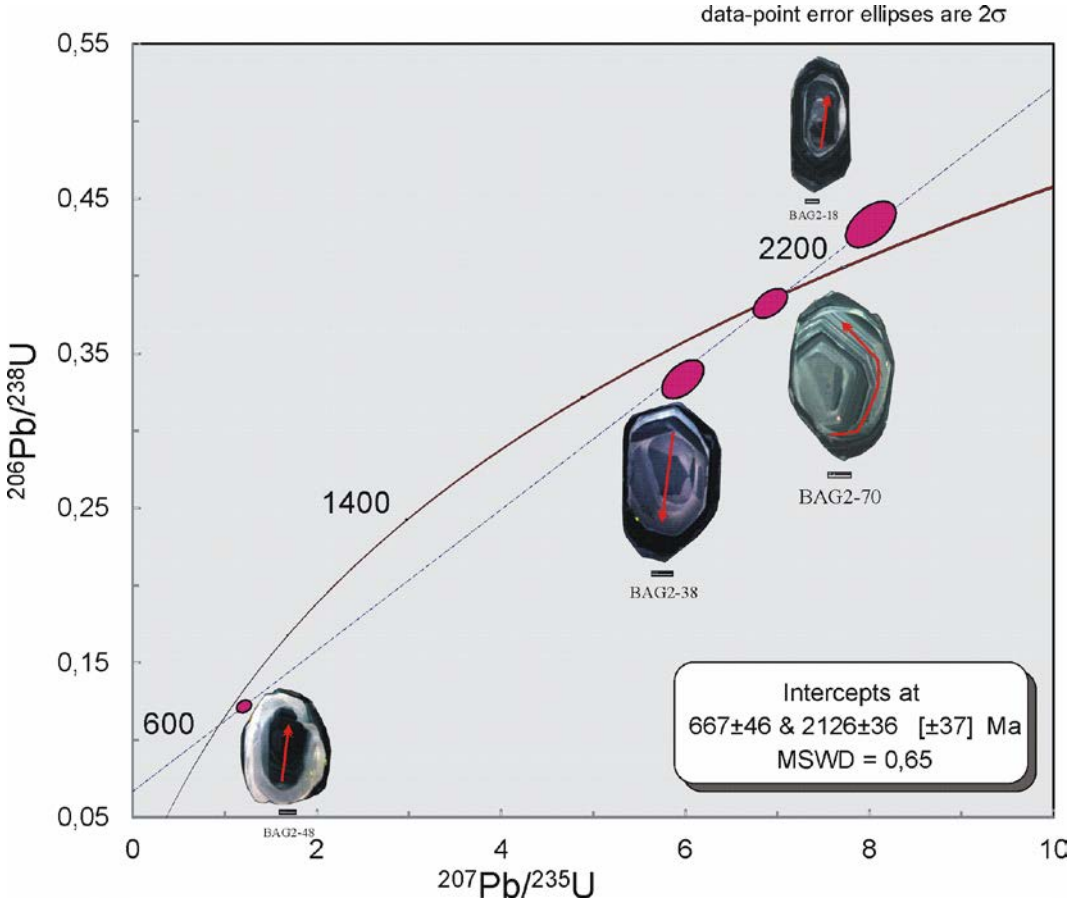

Figure 9. Concordia plot with the data of group 1 zircons of BAG2 granite sample

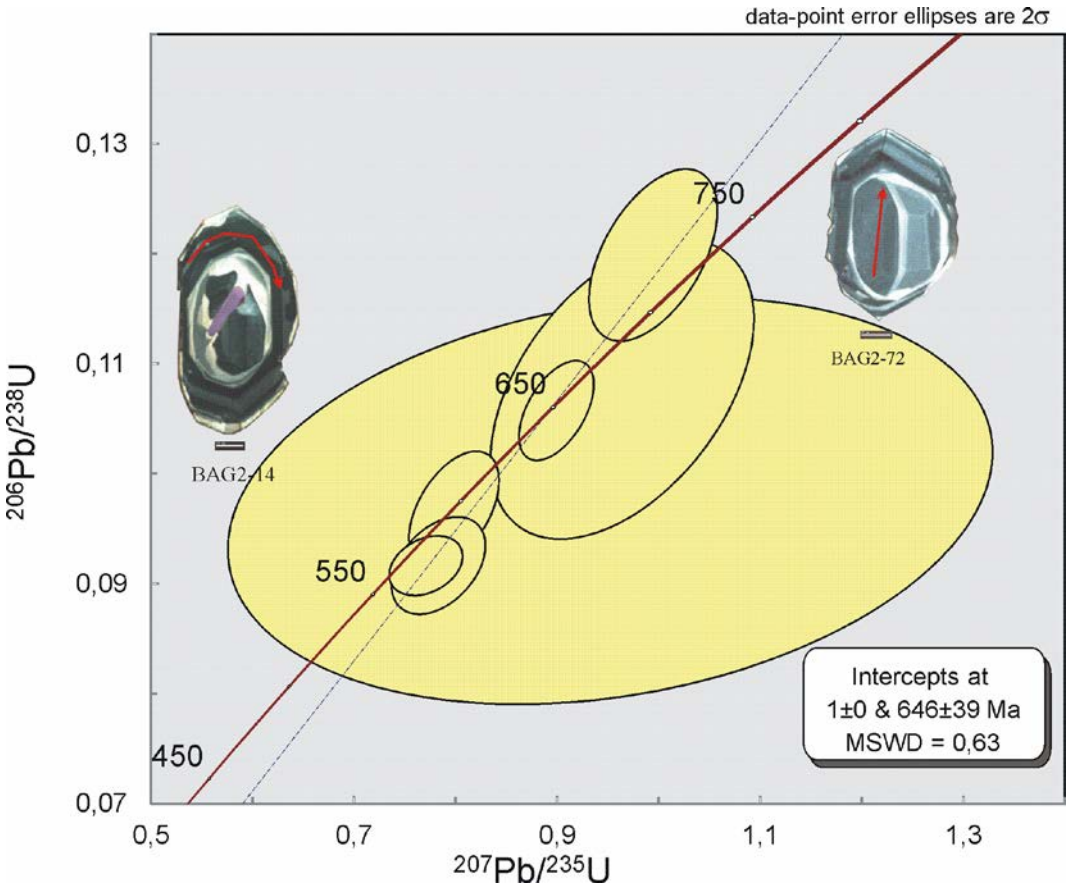

Figure 10. Concordia plot with the data of group 2 zircons of BAG2 granite sample

5. Discussions and Conclusion

The amphibole-biotite granite is characterized by granular texture made up of amphibole, biotite, feldspar, quartz, sphene, apatite and secondary mineral (chlorite, sericite). The brownish color of the biotite and the presence of sphene are significant of Ti in the original magma. ABG is characterized by zircon with well-developed oscillatory zonation. This zonation is inherited from the synmagmatic crystallization of the mineral. It expresses the cyclic accumulation of trace elements during the growth of the mineral in a melt [25]. The relative uniformity in the oscillatory zonation of the zircons means that they crystalize all in the same magmatic environment. Thus, the concordia age 607 ± 3 Ma from zircons of the LAO1 sample represents the crystallization age of the amphibole biotite granite. This value is at the error limit close to the mean age (601±1 Ma) obtained in the pyroxene-amphibole-biotite granite to the east of Meiganga and considered as dating its emplacement [3,5]. It is not unlikely that amphibole-biotite granite of Doua and pyroxene-amphibole-biotie granite of Meiganga are contemporaineous of the D3 deformational phase as mentioned by [1]. Contrary to the pyroxene-amphibole-biotite granite of Meiganga and Baibokoum with pyroxene, the amphibole-biotite granite under study has no pyroxene; it is important to note that the presence of pyroxene in such granite has been interpreted as xenocryst of the metamorphic basement [1,13]. One can deduce that the mineralogy hosted rock in the Doua area has no pyroxene.

The biotite-muscovite granite shows a granular to granular porphyritic texture with biotite, muscovite, plagiclas, K-feldspar, quartz, zircon, opaque minerals. The presence of two micas in the rock is indicative of its crustal origin. The faint schistosity observed in the BMG portrays its syn-tectonic character. Zircons of the biotite-muscovite granite show two domains, indicating that the evolution of the rock or minerals went through two different environments. The fact that the outer part is transgressing the inner part of the zircons (e.g. BAG2-12, BAG2-48) means that the outer part is formed by transformation of the preexisting zircon. Vavra et al., 1996, show that preexisting zircon can be transform during metamorphism. Th/U ratios of the zircons range from 0.22 to 1.07 except one value at 0.02 (BAG2-72); these values are typical of the magamatic zircon with respect to the lower limit (0.1) of the Th/U ratio define by Rubatto et al. [24,26]. The lower Th/U ration of zircon BAG2-72 can be explain by recrystallization during metamorphism as demonstrated by Hosking an black (2000). It is known that granitoids of central Cameroon are hosted in paleoproterozoic ortho- or para-derivative gneiss [1,22]. It is likely that the zircon grains which give ages of 2126 ±36 Ma (Upper intercept, cf Figure 10) and 667 ±46 Ma (Lower intercept, cf Figure 10) constitute xenocryst from the basement; may be from a paleoproterozoic granitoid emplaced at 2126 ±36 Ma or from sediments which detritus comes from such granitoids. The subconcordant zircons group with age of 646 ±39 Ma represent mineral of the biotite muscovite granite and thus date the crystallization of the magmatic body. The sub concordant character of these data could be linked to the recent lead lost as can be seen with the lower Anchored intercept at 1 ± 0.5 Ma (Cf Figure 10). While considering four zircon

grains (BAG2-02, BAG2-06, BAG2-72, BAG2-74) of this group, one obtains a discordia with an upper intercept at 657±57 Ma, the lower intercept being anchored at 1±0.5 Ma. The other three zircons (BAG2-14, BAG2-40 and BAG2-60) give concordant ages of 577±17Ma. It is not unlikely that the two ages correspond to two distinct tectonothermal events. The age 657±57 Ma is obtain in the inner domain of zircon with dominantly sector zonation (e.g. BAG2-72, cf. Figure 10). This value is at the error limit similar to the crystallization age of the amphibole-biotite granite LAO1, 607 ±3 Ma. It can therefore be regarded as dating the generation of the biotite-muscovite granite. The concordant age at 577±17 Ma is obtained at the border of the zircons (e.g. BAG2-14, cf. Figure 10) showing blurred oscillatory zonation. This feature means that the original magmatic oscillatory zonation was later blurred during a tectonic event. The tectonic event may be the latest activity of the CCSZ, characterized by dextral slip and which were though not older than 558±2 Ma ($^{207}Pb/^{206}Pb$ zircon evaporation age) by Ganwa et al. ([3]). The crystallization age of the granite is at the error limit similar to the lower intercept of the xenocrystal zircons which corresponds to the age of the metamorphism they suffer later. It is likely that biotite and muscovite granite is a syn metamorphic granite. This granite may originate from the anatectic melt of crustal material. The age 646 ±39 Ma may date not only the crystallization of the granite, but also the ultimate stage of metamorphism in the area with intense migmatization. Two micas granite is generally peraluminous rocks which occur in a variety of tectonic environment: closing back-arc basin environments, continental belts inboard of active arcs, active accretionary prism, continent-continent collision, large-scale shear zones associated with continental collision [10,12,23,33].

In fact, [4] associated the sinistral movement of the CCSZ to syn-D2 magmagenesis of the Meiganga metadiorite in the meantime of 614-619 Ma ($^{207}Pb/^{206}Pb$ zircon evaporation age), while the right lateral wrench movement was bracketed between 585 and 540 Ma [14], which is younger than the age of the granite. In Cameroon, the early tectonic evolution of the central Africa Fold Belt involve thrusting and shortening that leads to the crustal thickening between 630-620 Ma [14]. The age of the biotite-muscovite granite is at the error limit similar to the age of the thrusting event date at 630 ±5 Ma in the Poli micaschist [31], and at 620 ±10 Ma in the Yaoundé granulite [21]. It is not unlikely to consider that the studied biotite-muscovite granite was trigger because of the pre-D2 (perhaps syn-D1) activity of the CCSZ at 647 ±46 Ma in association with the collisional process. The natures of the movement of the CCSZ at that time, as well as the imprints of the movement in the basement need to be target.

Acknowledgements

This research was supported by the Austrian Science Fund (FWF), project M 1371-N19, who funded the stay of Ganwa Alembert Alexandre at the University of Vienne. We thank Franz Biedermann of the University of Vienna, Magdalena Mandl of Karls-Frazens Universität Graz, and Dorothee Hippler of Technische Universität Graz for technical assistance. Thanks go to anonymous reviewers for their critical comments on the manuscript.

References

[1] Ganwa, A.A. (2005). Les granitoïdes de Méiganga: étude pétrographique, géochimique, structurale et géochronologique. Leur place dans la chaîne panafricaine. Thèse de doctorat d'Etat, Univ. Ydé I, 162p.

[2] Ganwa, A.A., Frisch, W., Siebel, W., Ekodeck, G.E., Shang Kongyuy, C., Ngako, V. (2008). Archean inheritances in the pyroxene–amphibole-bearing gneiss of the Méiganga area (Central North Cameroon): Geochemical and $^{207}Pb/^{206}Pb$ age imprints. *Comptes Rendus Geoscience*, 340, 211-222.

[3] Ganwa, A.A., Siebel, W., Frisch, W., Shang Kongnyuy, C. (2011a): Geochemistry of magmatic rocks and time constraints on deformational phases and shear zone slip in the Méiganga area, central Cameroon. *International Geology Review*, Vol. 33, N° 7, June 2011, 759-784.

[4] Ganwa, A. A., Siebel, W., Frisch, W., Shang, C. K. and Ekodeck, G. E. (2011b). Geochemistry and geochronology of the Méiganga metadiorite: implications on the timing of D2 deformational phase in Adamawa Yadé Domain in Cameroon. *Int. J. Biol. Chem. Sci.* 5(4): 1754-1767, August 2011.

[5] Ganwa, A.A., Klötzli, U.S., Hauzenberger, C. (2016). Evidence for Archean inheritance in the pre-Panafrican crust of Central Cameroon: Insight from zircon internal structure and LA-MCICP-MS U-Pb ages. Journal of African Earth Sciences 120 (2016) 12-22.

[6] Hoskin, P.W.O., Black, L.P. (2000). Metamorphic zircon formation by solid-state recrystallization of protolith igneous zircon. J. Metamorph. Geol. 18, 423e439.

[7] Klötzli, E., Klötzli, U.,Kosler, J. (2007). A possible laser ablation xenotime U–Pb age standard: reproducibility and accuracy. Geochimica et Cosmochimica Acta 71, A495-A495.

[8] Klötzli, U., Klötzli, E, Günes, Z. and Kosler, J. (2009). Accuracy of Laser Ablation U-Pb Zircon Dating: Results from a Test Using Five Different Reference Zircons. Geostandards and Research Geoanalytical, Vol.33, N°1, 5-15.

[9] Lasserre, M. (1961). Etude géologique de la partie orientale de l'Adamaoua (Cameroun Central) et les principales sources minéralisées de l'Adamaoua. Bulletin de la Direction des Mines et Géologie du Cameroun, 4: 131p.

[10] Le Fort, P. (1981). Manaslu leucogranite: a collision signature of the Himalaya. A model for its genesis and emplacement. *J. Geophys. Res. 86*, 10545-iO568.

[11] Ludwig, K.R. (2003). User's manual for Isoplot/Ex version 3.00, a geochronological toolkit for Microsoft Excel. Berkeley Geochronology Center Special Publications, 4, 72pp.

[12] MCKENZIE, C.B. & CLARKE, D.B. (1975). Petrology of the South Mountain Batholith, Nova Scotia. *Can. J. Earth Sci.* 12, 1209-1218.

[13] Naïmou Seguem, Ganwa, A.A., Klötzli, U., Diguim Kepnamou, A., Ekodeck, G.E. (2014). Petrography and Geochemistry of Precambrian Basement Straddling the Cameroon-Chad Border: The Touboro Baïbokoum Area. International Journal of Geosciences, 2014, 5, 418-431.

[14] Ngako, V., Affaton, P., Njonfang, E. (2008). Pan-African tectonics in northwestern Cameroon: Implication for the history of western Gondwana. Gondwana Research 14 (2008) 509-522.

[15] Ngako, V., Affaton, P., Njonfang, E. (2009). Reply Pan-African tectonics in northwestern Cameroon: Implication for the history of western Gondwana. Gondwana Research 16 (2009) 165-166.

[16] Ngnotué, T., Nzenti, J.P., Barbey, P., Tchoua, F.M., 2000. The Ntui Bétamba high-grade gneisses: a northward extension of the panafrican Yaoundé gneisses in Cameroon. Journal of African Earth Sciences 31, 369-381.

[17] Njanko, T., Nédélec, A., Affaton, P. (2006). Synkinematic high-K calc-alkaline plutons associated with the Pan-African Central Cameroon Shear Zone (WTibati area): petrology and geodynamic significance. Journal of African Earth Sciences 44, 494-510.

[18] Nzenti, J.P. (1994). L'Adamaoua panafricain (région de Banyo) une zone clé pour un modèle géodynamique de la chaîne panafricaine nord équatoriale au Cameroun. *Thèse Doct. d'Etat Univ.Cheick Anta Diop-Univ de Nancy I.176p*.

[19] Nzenti, J.P., Kapajika, B., Wörner, G., Lubala, T.R., (2006). Synkinematic emplacement of granitoids in a Pan-African shear zone in Central Cameroon. Journal of African Earth Sciences 45, 74-86.

[20] Penaye, M.P., Toteu, S.F., Michard, A., Bertrand, J.M. And Dautel, D. (1989). Reliques granulitiques d´âge Protérozoïque inférieur dans la zone mobile panafricaine d´Afrique Centrale au Cameroun; géochronologie U/Pb sur Zircons. *Comptes Rendus de l´Académie Sciences* 309, 315-318.

[21] Penaye, J., Toteu, S.F., Van Schmus, W.R., Nzenti, J.P., (1993). U–Pb and Sm–Nd preliminary geochronologic data on the Yaoundé series, Cameroon: reinterpretation of the granulitic rocks as the suture of a collision in the "Centrafrican" belt. Comptes Rendus de l'Académie des Sciences, Paris 317, 789-794.

[22] Penaye, J., Toteu, S.F., Tchameni, R., Van Schmus, W.R., Tchakounte, J., Ganwa, A., Miyem, D., Nsifa, E.N. (2004). The 2.1 Ga West Central African Belt in Cameroon: extension and evolution. J. Afr. Earth Sci. 39, 159-164.

[23] Rottura, A., Caggianelli, A, Campana, R. and Del Moro, A. (1993). Petrogenesis of Hercynian peraluminous granites from the Calabrian Arc, Italy. *Eur. J. Mineral.* 5, 737-754.

[24] Rubatto, D., Williams, I.S., Buick, I.S. (2001). Zircon and monazite response to prograde metamorphism in the Reynolds Range, central Australia. Contrib Mineral Petrol (2001) 140: 458-468.

[25] Rubatto, D. (2002). Zircon trace element geochemistry: partitioning with garnet and the link between U–Pb ages and metamorphism. Chemical Geology 184 (2002) 123-138.

[26] Rubatto, D., Hermann, J., Berger A., Engi, M. (2009). Protracted fluid-induced melting during Barrovian metamorphism in the Central Alps. Contrib Mineral Petrol (2009) 158: 703-722.

[27] Sláma, J., Kosler, J., Condon, D.J., Crowley, J.L., Gerdes, A., Hanchar, J.M., Horstwood, M.S.A., Morris, G.A., Nasdala, L., Norberg, N., Schaltegger, U., Schoene, B., Tubrett, M.N. and Whitehouse, M.J. (2008). Plesovice zircon - A new natural reference material for U-Pb and Hf isotopic microanalysis. Chemical Geology, 249, 1-35.

[28] Stacey, J. S., Kramers, J. D. (1975). Approximation of terrestrial lead isotope evolution by a two-stage model. Earth Planet. Sci. Lett. 26, 207-221.

[29] Sylvester, P.J., Ghaderi, M. (1997). Trace element analysis of scheelite by excimer laser ablation-inductively coupled plasma-mass spectrometry (EELA-ICP-MS) using a synthetic silicate glass standard. Chemical Geology, 141, 49-65.

[30] Tchameni, R., Pouclet, A., Penaye, J., Ganwa, A.A., Toteu, S.F. (2006). Petrography and geochemistry of the Ngaoundéré Pan-African granitoids in Central North Cameroon: Implications for their sources and geological setting. *Journal of African Earth Sciences* 44 (2006) 511-529.

[31] Toteu, S.F., Macaudière, J., Bertrand, J.M., Dautel, D., 1990. Metamorphic zircons from northern Cameroon: implications for the Pan-African evolution of central Africa. Geologisch Rundschau 79, 777-786.

[32] Toteu S. F., Penaye, J. and Djomani, Y. P. (2004). "Geodynamic Evolution of the Pan-African Belt in Central Africa with Special Reference to Cameroon," *Canadian Journal of Earth Sciences*, Vol. 41, No. 1, January 2004, pp. 73-85.

[33] WHITE, A.J.R. & CHAPPELL, B.W. (1983). Granitoid types and their distribution in the Lachlan Fold Belt, southeastern Australia. *Geol. Soc. Am., Mem.* 159, 21-34.